^{169}Tm Mossbauer investigation of thulium pyrogermanate

1992 J. Phys.: Condens. Matter 4 1849

(http://iopscience.iop.org/0953-8984/4/7/023)

J. Phys.: Condens. Matter 4 (1992) 1849–1858. Printed in the UK

^{169}Tm Mössbauer investigation of thulium pyrogermanate

G A Stewart†, J M Cadogan‡ and A V J Edge†

† Department of Physics, University College, The University of New South Wales, Australian Defence Force Academy, Campbell, ACT 2600, Australia

‡ School of Physics, The University of New South Wales, Kensington, NSW 2033, Australia

Received 20 May 1991, in final form 18 October 1991

Abstract. A ^{169}Tm Mössbauer investigation of thulium pyrogermanate is reported. All spectra recorded over the temperature range 4.2 K–740 K are pure quadrupole doublets. This observation and the detailed temperature dependence of the quadrupole interaction are inconsistent with recent claims of a fivefold local symmetry at the Tm^{3+} site. Initial attempts at analysing the data in terms of the full crystal-field Hamiltonian appropriate for C_1 symmetry suggest that the electronic ground state consists of a pair of non-magnetic singlets well isolated from the next state.

1. Introduction

The series of tetragonal rare-earth pyrogermanates (RPG), having formula $R_2Ge_2O_7$ (R = rare earth) and space group $D_4^4/P4_12_12$ [1, 2], is unusual in that the rare-earth site is coordinated by seven oxygens which form a distorted pentagonal bipyramid. The local symmetry of the rare-earth 8b site is triclinic $C_1(1)$. Nevertheless, when the oxygen ligands are viewed along the *c*-axis (figure 1(*a*)), their arrangement appears to exhibit

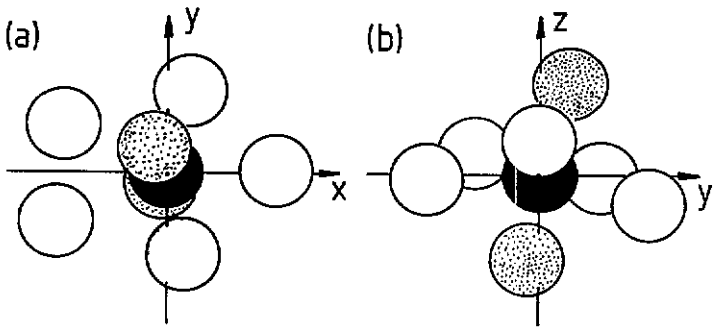

Figure 1. Coordination polyhedron of oxygen atoms about the Tm^{3+} site at fractional position 0.876, 0.353, 0.136 in TmPG: (*a*) viewed along the *c* axis; (*b*) side view. The thulium atom is solid black and two of the oxygen atoms are shaded to distinguish them from the five oxygen atoms comprising the basal plane of the distorted pentagonal bipyramid.

fivefold rotational symmetry. It is because of this that optical spectroscopy data for ErPG and DyPG [3] and magnetic susceptibility data for TmPG [4] have been analysed elsewhere in terms of a crystal-field (CF) Hamiltonian appropriate for the D_{5h} symmetry of an ideal pentagonal bipyramid. However, when viewed from a direction perpendicular to the c-axis (figure 1(b)), it is evident that the pentagonal bipyramid is far from ideal.

The prime reason for assuming a CF Hamiltonian corresponding to the higher D_{5h} symmetry is that only four CF parameters are required instead of the 27 required by C_1 symmetry (see (1) below). In similar vein, it is not uncommon for researchers to ignore all but the lowest rank ($n = 2$) CF parameters or to ignore all but the axial ($m = 0$) CF parameters. Although such approaches can prove useful, it is important to recognize that the predicted CF level scheme may not correctly reflect the local site symmetry. For example, Tm^{3+} is a non-Kramers ion whose $^3H_6$ ground term is split into 13 non-magnetic singlet states by a triclinic CF environment. By contrast, the assumption of a D_{5h} symmetry CF environment allows five magnetic doublets in addition to three non-magnetic singlets. The present ^{169}Tm Mössbauer investigation of TmPG has been carried out in response to a recent paper by Sengupta *et al* [5] in which a mixed magnetic-quadrupole interaction is predicted for ^{169}Tm in TmPG on the basis of their earlier fivefold-symmetry CF analysis [4]. An alternative semi-empirical analysis will be employed in an initial attempt to characterize the full triclinic symmetry of the Tm^{3+} site. Simple point-charge model (PCM) calculations of CF parameter ratios within each rank will be used to reduce to three the number of CF parameters actually fitted to the data.

2. Theoretical background and CF parameter ratios

For triclinic (C_1) site symmetry, the CF Hamiltonian for the $^3H_6$ ground term of Tm^{3+} in TmPG is written

$$H_{CF} = \sum_{\substack{n=2,4,6 \\ m=0,\pm1,\ldots,\pm n}} B_n^m O_n^m = \sum_{\substack{n=2,4,6 \\ m=0,\pm1,\ldots,\pm n}} C_n^m \theta_n O_n^m(J) \tag{1}$$

where C_n^m are the CF parameters and the θ_n are factors associated with the Stevens equivalent operators, $O_n^m(J)$ [6]. As a result of the CF interaction, there are two contributions to the electric field gradient (EFG) at the thulium nucleus [7]. The first is the temperature-dependent self-ion contribution brought about by the CF distortion of the 4f shell and the second is the constant lattice EFG representing the direct action of the CF at the nucleus. These contributions add [8] to produce total EFG components

$$V_{ij} = (-\theta_2 e/4\pi\varepsilon_0)\langle r^{-3}\rangle_{4f}(1 - R_Q)F_2^m\langle O_2^m(J)\rangle_T + [-4(1 - \gamma_\infty)/e(1 - \sigma_2)\langle r^2\rangle_{4f}]L_2^m C_n^m \tag{2}$$

where R_Q, γ_∞ and σ_2 are the atomic shielding, Sternheimer antishielding and CF shielding parameters respectively. The factors L_2^m and F_2^m relevant to triclinic symmetry are listed in table 1. The total EFG tensor must be diagonalized to derive $V_{z'z'}$ and the asymmetry parameter

$$\eta' = \frac{(V_{x'x'} - V_{y'y'})}{V_{z'z'}}$$

with respect to the principal axes. The temperature-dependent quadrupole splitting, $\Delta E_Q(T)$, of the ^{169}Tm, $I = \frac{3}{2}$ level is then given by

$$\Delta E_Q(T) = (eQV_{z'z'}/2)(1 + \eta'^2/3)^{1/2} \tag{3}$$

where Q is the level's quadrupole moment. The theory is least-squares-fitted to the

Table 1. EFG tensor components and factors required in equation (2) for local C_1 (triclinic) symmetry.

m	ij	L_2^m	F_2^m
0	zz	1	1
+1	zx	$\frac{1}{4}$	3
−1	yz	$\frac{1}{4}$	3
+2	$xx - yy$	1	3
−2	xy	$\frac{1}{4}$	$\frac{3}{4}$

temperature-dependent quadrupole splitting data by systematic variation of the CF parameters and the 'shielding' parameters,

$$\rho_1 = Q(1 - R_Q)\langle r^{-3}\rangle_{4f} \tag{4a}$$

and

$$\rho_2 = Q(1 - \gamma_\infty)/[(1 - \sigma_2)\langle r^2\rangle_{4f}] \tag{4b}$$

which collect those terms from equations (2) and (3) that need to be calculated theoretically or determined experimentally.

Simple PCM calculations are notoriously unsuccessful at predicting absolute CF parameter values, even for highly ionic materials. Nevertheless, such calculations can sometimes provide useful first estimates of the relative magnitudes of CF parameters within any given rank. Therefore, in order to reduce from 27 to 3 the number of independent CF parameters requiring to be fitted, two different types of PCM calculations have been employed for the determination of CF parameter ratios

$$r_2^m = C_2^m/C_2^0 \qquad r_4^m = C_4^m/C_4^0 \qquad r_6^m = C_6^m/C_6^0.$$

In the first approach (approach A), only the seven oxygen ligands were considered. Despite the fact that the rank $n = 2$ CF interaction is long range, this approach recently proved remarkably successful for the ceramic high-temperature superconductors, $RBa_2Cu_3O_{7-\delta}$ [9]. In the second approach (approach B), the PCM summation was over all Tm^3, Ge^{4+} and O^{2-} within a sphere of radius $20\,a_0$, centred on Tm^{3+}. All PCM calculations were performed specifically for the Tm^{3+} site shown in figure 1 with x-, y- and z-axes chosen to align with the a-, b- and c-crystallographic axes respectively. TmPG lattice parameters and atomic position parameters were taken from the structural determination by Stadnicka *et al* [2]. Both sets of PCM-calculated ratios (together with the PCM-calculated C_n^0) are presented in table 2. Given the hazardous nature of the point charge assignment for approach B, the two sets of ratios are in surprisingly good agreement for the higher ranks ($n = 4, 6$). Although the r_2^m magnitudes are in rough agreement, they are dominated by a sign change in the PCM-calculated C_2^0. For the purpose of comparison, the CF parameters resulting from the D_{5h} symmetry analysis of Sengupta *et al* [4] have been converted to Stevens notation and included in table 2.

3. Experimental details

An initial specimen (specimen 1) of TmPG was prepared from a stoichiometric mix of Tm_2O_3 and GeO_2 that was pressed into a cylindrical pellet and calcined for two days at

Table 2. Shielding and CF parameters corresponding to the theoretical curves of figure 4.

	C_1 (approach A)		C_1 (approach B)		D_{5h} [4]
	PCM	expt.[a]	PCM	expt.[a]	expt.[b]
C_2^0 (cm^{-1})	−54.3	−88.2	+39.2	+55.8	+384.3
r_2^1	−12.0		+14.5		
r_2^{-1}	+1.02		−4.56		
r_2^2	+5.49		−11.8		
r_2^{-2}	+3.18		−5.77		
C_4^0 (cm^{-1})	+102.5	+390.4	+85.1	+286.9	+332.4
r_4^1	−0.94		−0.96		
r_4^{-1}	+3.88		+4.08		
r_4^2	+0.42		+0.98		
r_4^{-2}	+0.56		+0.57		
r_4^3	+7.94		+7.78		
r_4^{-3}	+0.23		+0.71		
r_4^4	+2.84		+2.53		
r_4^{-4}	−0.33		−4.65		
C_6^0 (cm^{-1})	+5.0	−14.8	+6.2	−2.5	+19.57
r_6^1	+1.04		+0.63		
r_6^{-1}	+7.02		+5.49		
r_6^2	−4.53		−3.88		
r_6^{-2}	−4.14		−3.46		
r_6^3	−8.74		−7.91		
r_6^{-3}	+1.57		+1.32		
r_6^4	+0.76		+1.42		
r_6^{-4}	−1.02		−0.95		
r_6^5	+4.11		+1.87		−394.9
r_6^{-5}	−8.19		−6.33		
r_6^6	−10.3		−10.3		
r_6^{-6}	−1.43		−1.32		
ρ_1 (b au^{-3})		−15.2[c]		−15.2[c]	−15.2[c]
ρ_2 (b au^{-2})		−314.4		−305.2	−381[d]
Δ (cm^{-1})		11.1		16.7	
Δ' (cm^{-1})		188		150	

[a] C_n^m ($m \neq 0$) set equal to r_n^m (PCM) C_n^0.
[b] Converted from [4] using table 4 of Morrison and Leavitt [14].
[c] As recommended by Stewart *et al* [11].
[d] Theoretical value based on $Q = -1.5$ b [12], $(1 - \gamma_\infty) = 59.8$ [13] and $(1 - \sigma_2)\langle r^2 \rangle_{4f} = 0.236$ au^2 [13].

1100 °C. X-ray powder diffraction analysis revealed a substantial GeO_2 impurity phase (figure 2(*a*)), which was subsequently removed by two further heat treatments (figures 2(*b*)–(*c*)), producing specimens 2 and 3. For each additional heat treatment, the material was reground, pelletized and calcined for two days at 1150 °C. As well as removing the GeO_2 impurity phase, the additional heat treatments brought the intensities of the 210 and 202 x-ray reflections into line with those observed elsewhere [10] for isostructural ErPG.

The ^{169}Tm single-line source was prepared by neutron irradiation of a 20 mg, 13 mm diameter $^{168}Er_{1.5}Al_{98.5}$ disc. TmPG absorbers of approximately 7 mg cm^{-2} were cooled in

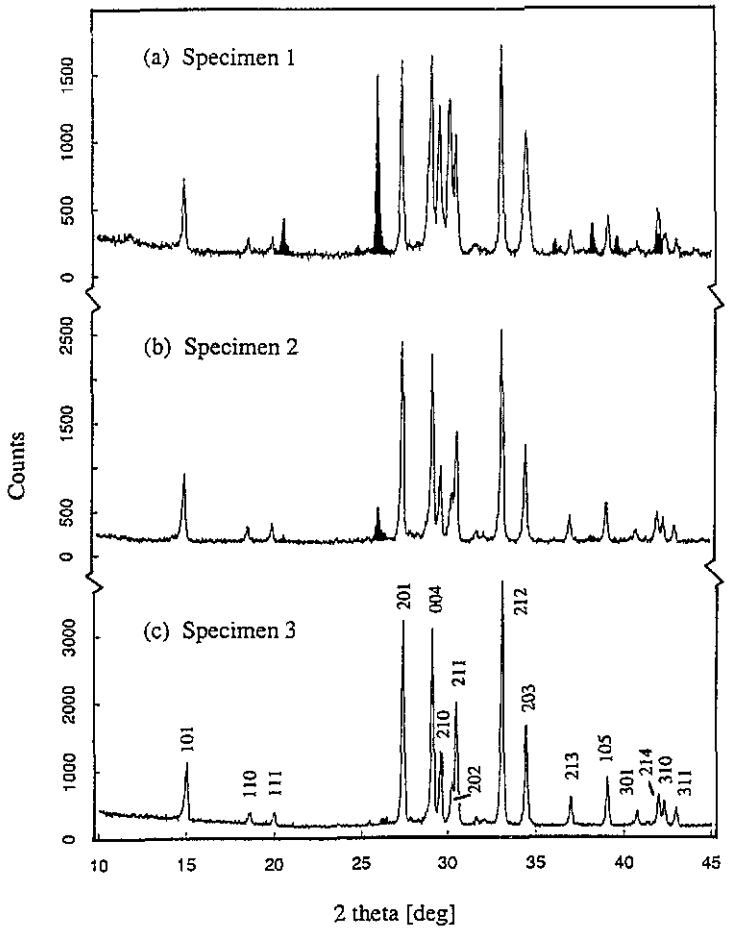

Figure 2. Cu K_α x-ray powder diffraction patterns for the three TmPG specimens.

a transmission cryostat or heated in a transmission furnace. The source was mounted outside at room temperature on a sinusoidal motion drive.

4. Results and discussion

^{169}Tm Mössbauer spectra were recorded for specimen 1 over the temperature range 4.2–300 K and for specimen 3 over the temperature range 4.2–740 K. Figure 3 shows a selection of specimen 3 spectra at 4.2 K, 300 K and 740 K, together with the specimen 1 spectrum at 300 K. The improved statistics of the two room-temperature spectra are due to the fact that they were recorded 'on the bench' with a reduced source-to-absorber separation and in the absence of strong 8.4 keV γ-ray absorption by either cryostat or oven windows. All of the Mössbauer spectra in the temperature range 4.2–300 K were able to be interpreted as pure quadrupole-split Lorentzian doublets. However, it was necessary to allow a weak line-width asymmetry and, for temperatures less than 100 K, the quadrupole splitting was significantly larger for specimen 3 than for specimen 1.

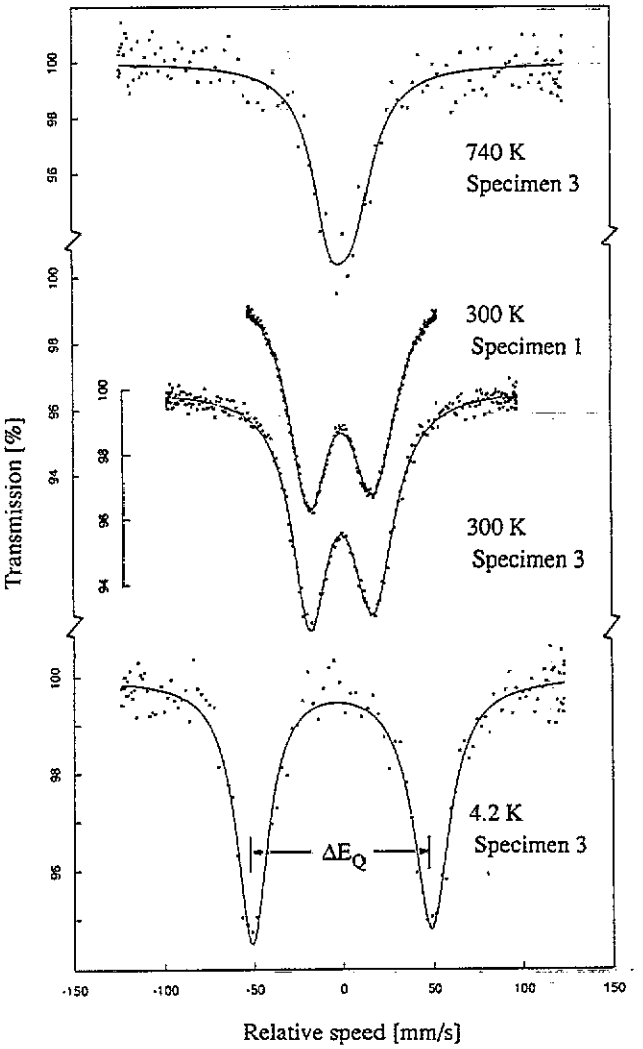

Figure 3. Representative ^{169}Tm Mössbauer spectra for TmPG.

Parameters fitted to the spectra of the two specimens at 4.2 K and 300 K are compared in table 3. The high-temperature ($T > 300$ K) spectra recorded for specimen 3 were analysed assuming constant line-widths identical to those fitted at 300 K. At the conclusion of the high-temperature measurements, a further spectrum was recorded at 4.2 K to check that the prolonged furnacing had not modified the specimen. Figure 4 shows the quadrupole splittings determined for both specimens as a function of temperature. The error bars for the high-temperature results refer to the fit as described above and do not include any additional error associated with the assumed line-widths.

The difference between the low-temperature quadrupole splittings determined for specimens 1 and 3 is intriguing. Apart from the slightly larger linewidths fitted for specimen 1 (see table 3), the ^{169}Tm Mössbauer spectra are well resolved for both specimens and there is no evidence for Tm phases other than TmPG. ^{169}Tm Mössbauer

Table 3. Comparison of half-width-half-maximum linewidths, $\Gamma/2$, and quadrupole splittings, ΔE_Q, fitted to the ^{169}Tm Mössbauer spectra for specimens 1 and 3 at room temperature and at liquid helium temperature.

T (K)	Specimen	$\Gamma/2$ (mm s^{-1}) ($v<0$)	$\Gamma/2$ (mm s^{-1}) ($v>0$)	ΔE_Q (mm s^{-1})
300	1	13.4(3)	15.2(1)	35.36(8)
	3	12.0(3)	13.5(3)	34.6(2)
4.2	1	15.4(6)	16.6(6)	92.3(5)
	3	10.7(7)	12.6(9)	99.7(7)

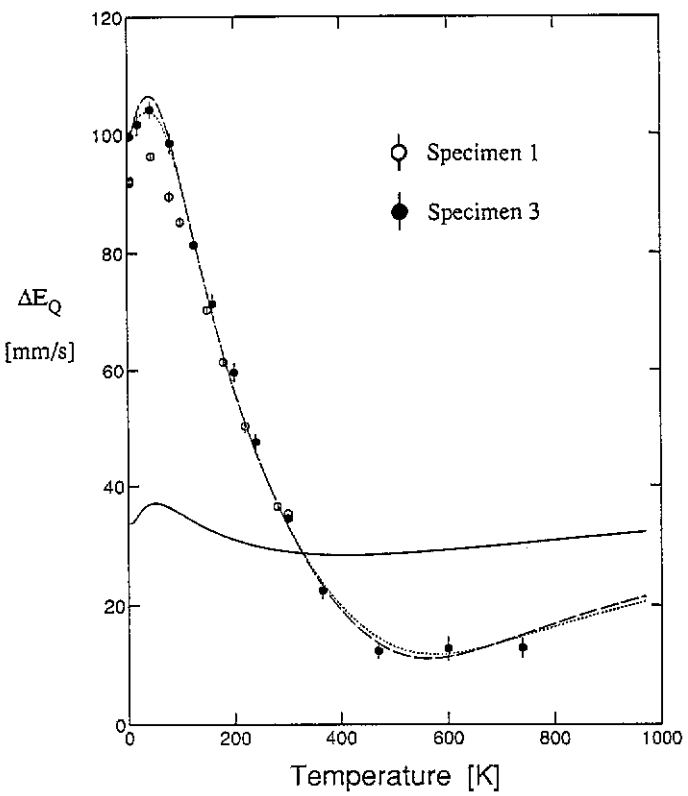

Figure 4. Quadrupole splitting, ΔE_Q, as a function of temperature for the $I = \frac{3}{2}$ nuclear level of ^{169}Tm in TmPG. The theoretical curves correspond to the D_{5h} symmetry CF parameters of [4] (full curve) and this work's full C_1 symmetry, semi-empirical approaches A (dotted curve) and B (broken curve).

spectroscopy is a microscopic technique and the TmPG phase should not be influenced by the coexistence of a GeO_2 phase resulting from incomplete solid-state reaction. Hence the CF parameters for the TmPG phase of specimen 1 must differ from those for the TmPG phase of specimen 3. Since neither the x-ray powder diffraction nor the ^{169}Tm

Mössbauer spectroscopy reveals a Tm-rich counterpart to the unreacted GeO_2 impurity phase of specimen 1, one might conjecture that its TmPG phase is germanium-depleted. An associated disorder could be responsible for the small increase in linewidths and the poorer fit to the saddle of the 300 K spectrum shown in figure 3. On average, the germanium atoms of the TmPG structure are located approximately 50% further from the Tm site than the nearest-neighbour oxygen atoms of the distorted pentagonal bipyramid. Hence germanium depletion would be expected to exert only minimal influence on the CF parameters (in particular the higher order CF parameters). Nevertheless, the quadrupole interaction at the ^{169}Tm nucleus is particularly sensitive to CF perturbations at low temperatures, where only the ground states are populated and the EFG is dominated by the CF distortion of the 4f shell. A more detailed investigation of the x-ray diffraction spectra is currently under way to ascertain whether such a germanium depletion is consistent with the observed variation in intensities of the 210 and 202 x-ray reflections. The remainder of this discussion will be confined to specimen 3 results.

The magnetic-ordering temperatures and de Gennes factors for pyrogermanates of the neighbouring heavy rare earths are: 2.05 K, 10.5 (Tb); 2.15 K, 7.083 (Dy); 1.45 K, 4.5 (Ho); and 1.15 K, 2.55 (Er), respectively [15]. The extrapolated magnetic ordering temperature for TmPG, with a de Gennes factor of 1.167, is then 0.8 K. Hence it is unlikely that TmPG orders magnetically at 4.2 K (this is supported by the present measurements). However, the D_{5h} CF symmetry analysis of magnetic TmPG susceptibility data [4] yielded a magnetic doublet as the CF ground state of the paramagnetic Tm^{3+} ion. Accordingly, Sengupta *et al* [5] predicted a mixed magnetic-quadrupole hyperfine interaction and a six-line ^{169}Tm Mössbauer spectrum at 4.2 K. The present measurements contradict the D_{5h} CF symmetry predictions on two counts. Firstly, all ^{169}Tm Mössbauer spectra recorded in this investigation are simple quadrupole split doublets. There is no evidence for a six-line spectrum at 4.2 K. Secondly, supposing the magnetic hyperfine component is washed out by electronic relaxation at a rate that is rapid compared with the nuclear Larmor precession frequency, one would expect the temperature-dependence of the quadrupole splitting to be as predicted by the D_{5h} CF parameters. The full curve in figure 4 represents the quadrupole interaction calculated for the D_{5h} symmetry CF parameters of Sengupta *et al* [4]. Its temperature dependence agrees with that previously predicted for the self-ion contribution (figure 1 in [5]) but bears little resemblance to the present experimental results. For the purpose of this calculation, the recommended value of $\rho_1 = -15.2$ b au^{-3} [11] was assumed and the second shielding parameter was fixed at the 'theoretical' value of $\rho_2 = -381$ b au^{-2}. Note, however, that the temperature dependence of the curve is not influenced by the value of ρ_2, the variation of which serves only to displace the curve vertically. The D_{5h} symmetry calculations represent a special axially symmetric ($\eta = 0$) case of the theory described in section 2, so that the total quadrupole splitting is a straightforward sum of the quadrupole splittings computed independently for the lattice and the 4f EFG contributions. Based on these arguments, it is proposed that the D_{5h} CF symmetry approximation is invalid and that a full triclinic C_1 symmetry must apply.

The broken lines included in figure 4 correspond to full C_1 symmetry, semi-empirical fits in which the ratios r_n^m ($m \neq 0$) were fixed as determined for PCM calculation approaches A and B. The fitted values of the remaining three independent CF parameters C_2^0, C_4^0 and C_6^0 and the second shielding parameter, ρ_2, are included in table 2. The first shielding parameter was fixed at the recommended value of $\rho_1 = -15.2$ b au^{-3} [11]. Despite the approximate agreement between the higher-rank ($n = 4, 6$) ratios calculated for the two PCM approaches, the fitted sets of parameters C_2^0, C_4^0 and C_6^0 differ considerably. This is evidently brought about by the difference in the r_2^m ratios calculated for the

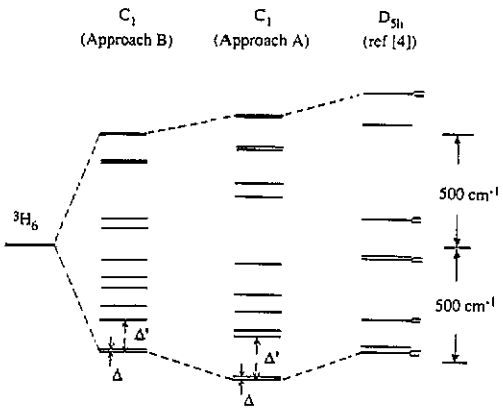

Figure 5. Ground term CF schemes for Tm^{3+} in TmPG corresponding to approaches A and B (this work) and the D_{5h} symmetry CF parameters [4].

two PCM approaches. Nevertheless, the ground-term CF schemes corresponding to the theoretical fits of approaches A and B (figure 5) exhibit definite similarities. Both approaches predict a low-lying pair of singlet ground states separated by $\Delta \simeq 15\ cm^{-1}$ and both approaches predict that this pair of singlet ground states will be well isolated ($\Delta' \geqslant 150\ cm^{-1}$) from the next excited level.

It is worth noting that asymmetric relaxation line broadening can result from the second-order magnetic hyperfine interaction associated with a pair of singlet ground states. However, such an effect is an unlikely origin of the weak line shape asymmetry observed for the specimen 3 ^{169}Tm Mössbauer spectra. Firstly, the so-called 'pseudo-quadrupole' effect theory of Clauser *et al* [16] predicts that both the spectrum asymmetry and the absolute line widths will increase with decreasing temperature. From table 3, the linewidths for specimen 3 are observed to be smaller at 4.2 K than at 300 K. Secondly, the effect typically requires a singlet separation of $\Delta < 5\ cm^{-1}$. In this regard, the semi-empirical CF analyses are consistent with the experimental observations.

5. Conclusion

The present ^{169}Tm Mössbauer investigation of TmPG demonstrates the assumption of a five-fold site symmetry to be invalid. Semi-empirical approaches have been employed to analyse the strong temperature dependence of the measured quadrupole splitting, ΔE_Q, in terms of the 27 CF parameters required for the C_1 symmetry. Although the effectiveness of such analyses is limited ultimately by the rank $n = 2$ CF ratio calculations, both approaches yielded ground-term CF schemes in which a pair of singlet ground states is well isolated from the next excited state.

Acknowledgments

This work was supported by a grant from the Australian Institute of Nuclear Science and Engineering. The authors are grateful to Associate Professor Campbell for the use of his transmission cryostat and furnace and to Associate Professor Creagh for the loan of essential nucleonics.

References

[1] Smolin Y I 1970 *Sov. Phys.–Crystallogr.* **15** 36–9
[2] Stadnicka K, Glazer A M, Koralewski M and Wanklyn B M 1990 *J. Phys.: Condens. Matter* **2** 4795–805
[3] Wardzynska M and Wanklyn B M 1977 *Phys. Status Solidi* a **40** 663–8
[4] Sengupta A, Dasgupta S, Ghosh D and Wanklyn B M 1988 *Solid State Commun.* **67** 745–7
[5] Sengupta A, Bhattacharyya S and Ghosh D 1989 *Phys. Lett.* **140A** 261–4
[6] Rudowicz C 1985 *J. Phys. C: Solid State Phys.* **18** 1415
[7] Barnes R G, Mössbauer R L, Kankeleit E and Poindexter J M 1964 *Phys. Rev.* A **136** 175
[8] Stewart G A 1985 *Hyperfine Interact.* **23** 1–16
[9] Furrer A, Brüesch P and Unternährer P 1988 *Phys. Rev.* B **38** 4616–23
Bergold M, Wortmann G and Stewart G A 1990 *Hyperfine Interact.* **55** 1205–11
[10] Larson F and McCarthy G 1987 *JCPDS Grant-in-Aid Report* 38–0290
[11] Stewart G A, Day R K, Dunlop J B and Price D C 1988 *Hyperfine Interact.* **40** 339–42
[12] Olesen M C and Elbek B 1960 *Nucl. Phys.* **15** 134
and equation (21) of
Bleaney B, Bowden G J, Cadogan J M, Day R K and Dunlop J B 1982 *J. Phys. F: Met. Phys.* **12** 795
[13] Gupta R P and Sen S K 1973 *Phys. Rev.* A **7** 850
[14] Morrison C A and Leavitt R P 1983 *Handbook on the Physics and Chemistry of Rare Earths* ed K A Gschneidner Jr and L Eyring (Amsterdam: North-Holland) p 219
[15] Wanklyn B M 1973 *J. Mater. Sci.* **8** 649
[16] Clauser M J and Mössbauer R L 1969 *Phys. Rev.* **178** 559
Noakes D R and Shenoy G K 1983 *Hyperfine Interact.* **15/16** 1029–32